SOILS AND FOUNDATIONS Vol. 29, No. 3, 41-53, Sept. 1989
Japanese Society of Soil Mechanics and Foundation Engineering

GENERAL THEORY OF SHEAR BANDS FORMATION BY A NON-COAXIAL CAM-CLAY MODEL

CHIKAYOSHI YATOMI[i], ATSUSHI YASHIMA[ii], ATSUSHI IIZUKA[iv]
and IKUO SANO[iii]

ABSTRACT

In order to simulate the formation of localized shear bands, which is commonly observed during large deformation of soils, we first present a systematic extension of the well known Cam-clay model developed for small strains to the model for finite strains/deformations and then incorporates a non-coaxial term in the model. Finally, confining the deformation to undrained plane strain conditions, we examine the effects of the non-coaxial term on the shear bands formation.

Key words : Cam-clay model, constitutive equations, finite deformations, non-coaxial, shear bands (**IGC** : E 3/D 6)

INTRODUCTION

The purpose of this paper is to give the theoretical basis to simulate the formation of localized shear bands, which is commonly observed during large deformation of soils (see, Photo. 1) ; for instance, the slip lines observed in the laboratory test specimen, the sliding failure of embankment foundation, and the fault caused by the orogenic movement. Such simulation of shear bands formation may lead to clarify the occurrence mechanism of their phenomena and also make it possible to explain the soil behavior consistently from the beginning of deformation up to the limit failure state.

Localization analyses on soil samples have been presented by Prevost and Hughes (1981) and Borst (1988). Yet, their analyses are restricted to small strains/deformations and, therefore, in order to have shear band bifurcation, materials are assumed to be the strain-softening elasto-plastic model or the hardening model with a non-associated flow rule. The behavior of clay is, however, well explained by the elasto-plastic model with an associated flow rule and the slip lines are usually observed before the peak load in the unconfined compression test ; hence, the observed softening seems to be a structural effect due to the development of shear bands rather than a material property.

i) Instructor, Dept. of Aeronautical Eng., Kyoto University, Kyoto 606.
ii) Instructor, Disaster Prevention Research Institute, Kyoto University, Uji, Kyoto 611.
iii) Instructor, Dept. of Civil Eng., Kyoto University, Kyoto 606.
iv) Instructor, Dept. of Civil Eng., Kanazawa University, Kanazawa 920.
Manuscript was received for review on May 11, 1988.
Written discussions on this paper should be submitted before April 1, 1990, to the Japanese Society of Soil Mechanics and Foundation Engineering, Sugayama Bldg. 4 F, Kanda Awaji-cho 2-23, Chiyoda-ku, Tokyo 101, Japan. Upon request the closing date may be extended one month.

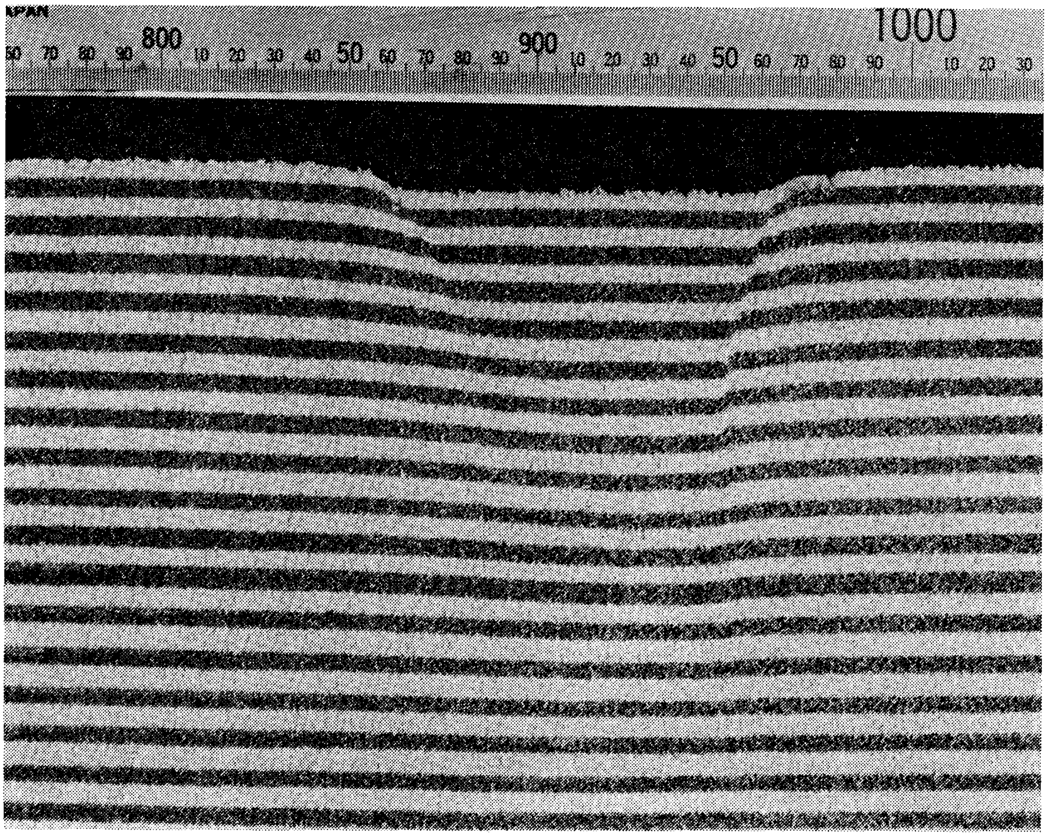

Photo. 1. Shear band formation (after Tani et al, 1987)

Prevost(1984) has presented the localization analysis for finite strains and showed that the localization could be captured in finite element models by employing, in the case of symmetrical configuration, an imperfection in the form of a weak element. However, introduction of such an imperfection in the material element would result in an artificial result. Also, the geometry of shear bands and the limit load which is found depend on the particular imperfection which is introduced.

This paper is concerned with a shear band analysis for finite strains/deformations in hardening materials and without introducing any imperfections in the material element ; therefore, the softening is here regarded as a consequence of the shear bands development and the development of shear bands is expected to occur naturally. The material employed here is the well-known Cam-clay model developed for small strains by Roscoe, Schofield and Thurairajah (1963), which is a coaxial hardening elasto-plastic model up to a critical state, that is, the principal directions of the plastic stretching are coaxial with those of the stress tensor. We then first extend the coaxial Cam-clay model developed for small strains to the model for finite strains.

However, as is explained in detail later, it is argued that the predictions from the coaxial model about the conditions at the initiation of shear bands are not in accordance with the experimental data and that in granular materials the existence of microscopic localized deformations may not result in coaxiality. In order to obtain the reasonable predictions, a number of writers then propose the non-coaxial models. We propose a new model which incorporates a non-coaxial term in the extended Cam-clay model, simply following the basic procedure of Rudnicki and Rice (1975).

Finally, confining the deformation to undrained plane strain conditions, we examine the effects of the non-coaxial term on the shear bands formation.

CAM-CLAY MODEL FOR FINITE STRAINS

We first present a systematic extension of the well known Cam-clay model developed for small strains to the model for finite strains and then incorporate a noncoaxial term in the model.

Coaxial Cam-Clay Model

It has been well recognized that the constitutive relations for saturated clays should be based on the *effective* (*Cauchy*) *stress tensor* $\boldsymbol{T}'$, which is defined by

$$\boldsymbol{T}'=\boldsymbol{T}+u\,\mathbf{1}.$$

Here, $\boldsymbol{T}$ is the *total Cauchy stress tensor*, u is the *pore water pressure*, and $\mathbf{1}$ is the unit tensor.

We then define the *effective mean normal stress* p' and the *generalized stress deviator* q as

$$p'=-\frac{1}{3}tr\boldsymbol{T}',$$

$$q=\sqrt{\frac{3}{2}}\|\boldsymbol{S}\|,$$

where $\boldsymbol{S}$ is the deviatoric part of $\boldsymbol{T}'$.

Note that, here and in what follows, we regard tension and extension positive and compression and contraction negative except u, p', and the volumetric strain v; an ordinary exchange of the sign in soil mechanics needs a special care and makes the discussion troublesome since stress rates employed in finite strain theory are not merely the rate of stress.

Consider a motion of a body $\boldsymbol{x}=\chi(\boldsymbol{X},t)$, and let $\boldsymbol{F}=\partial\boldsymbol{x}/\partial\boldsymbol{X}$ denote the *deformation gradient* corresponding to a given reference point $\boldsymbol{X}$. We assume that $\boldsymbol{F}$ is smooth with strictly-positive determinant;

$$J=det\,\boldsymbol{F}>0.$$

Then

$$\boldsymbol{L}=\dot{\boldsymbol{F}}\boldsymbol{F}^{-1},$$

is the *velocity gradient*,

$$\boldsymbol{D}=\frac{1}{2}(\boldsymbol{L}+\boldsymbol{L}^T),$$

the *stretching tensor*, and

$$\boldsymbol{W}=\frac{1}{2}(\boldsymbol{L}-\boldsymbol{L}^T),$$

the *spin tensor*.

We adopt the following decomposition;

$$\boldsymbol{D}=\boldsymbol{D}^e+\boldsymbol{D}^p. \tag{1}$$

Here superscript e stands for the elastic part, and superscript p for the plastic part.

Consider an isotropic consolidation. The increment in *void ratio* $\dot{e}$ associated with any increment of effective mean normal stress $\dot{p}'$ is given by

$$\dot{e}=-\lambda\frac{\dot{p}'}{p'},$$

and hence the *volumetric strain rate* is

$$\dot{v}(=-tr\boldsymbol{D}=-\dot{J}/J=\dot{e}/(1+e))$$
$$=\frac{\lambda}{1+e}\frac{\dot{p}'}{p'}, \tag{2}$$

where λ is the *compression index*. Similarly, for an isotropic swelling, we have

$$\dot{v}^e=\frac{\kappa}{1+e}\frac{\dot{p}'}{p'}, \tag{3}$$

where κ is the *swelling index*; then we call

$$\tilde{K}=\frac{1+e}{\kappa}p',$$

the *bulk modulus* and

$$\tilde{G}=\frac{3(1-2\nu)}{2(1+\nu)}\tilde{K}, \tag{4}$$

the *shear modulus* with ν as the *Poisson's ratio*. The volumetric strain rate for dilatancy is given by

$$\dot{v}^p=D\left(\frac{q}{p'}\right)^{\cdot}, \tag{5}$$

where D is the *coefficient of dilatancy*, which is related to the *critical state parameter* M as (Ohta, 1971)

$$D=\frac{\lambda-\kappa}{M(1+e)}.$$

Finally, by Eqs. (2), (3), and (5), the total volumetric plastic strain rate is

$$\dot{v}^p=\frac{\lambda-\kappa}{1+e}\frac{\dot{p}'}{p'}+D\left(\frac{q}{p'}\right)^{\cdot}.$$

Here we note that the void ratio e at the current time is not, in general, constant for finite strain theory and is related the void ratio e_0 at the reference time as

$$1+e=J\ (1+e_0)\ ;$$

besides, $J=det\boldsymbol{F}$ is given by $\boldsymbol{D}$ as

$$J=\exp\left(\int_0^t tr\boldsymbol{D}dt\right).$$

Similarly to the definition of the yield function in Cam-clay model for small strain theory (Roscoe, Schofield and Thurairajah, 1963), it is then natural to define the yield *functional* for finite strains in the form

$$f=\int_0^t\left(\frac{\lambda-\kappa}{1+e}\frac{\dot{p}'}{p'}+D\dot{\eta}\right)dt-v^p, \tag{6}$$

where $v^p=0$ at $t=0$, and $\eta=q/p'$. It is important to note that, under the undrained condition with $\mathrm{tr}\boldsymbol{D}=0$, we have $J\equiv1$ (i. e. $1+e=1+e_0$) ; hence, the integrand in (6) is integrable on the stresses and f becomes a (yield) function of the stresses as for small strain theory. Differentiating f with respect to t, we obtain

$$\dot{f}=N_{ij}\dot{T}'_{ij}-\dot{v}^p, \tag{7}$$

where, for simplicity, we set

$$N_{ij}=D\left(M\frac{1}{p'}\frac{\partial p'}{\partial T'_{ij}}+\frac{\partial\eta}{\partial T'_{ij}}\right),$$
$$=\frac{D}{p'}\left(\frac{3}{2\eta}\frac{S_{ij}}{p'}-\frac{1}{3}\beta\delta_{ij}\right),$$

with $\beta=M-\eta$.

We assume that the elastic part of stretching tensor $\boldsymbol{D}^e$ is related to the *co-rotational (Jaumann) rate of effective stress,*

$$\overset{\circ}{\boldsymbol{T}}{}'=\dot{\boldsymbol{T}}'-\boldsymbol{W}\boldsymbol{T}'+\boldsymbol{T}'\boldsymbol{W},$$

by means of a relation similar to Hooke's law :

$$\overset{\circ}{T}{}'_{ij}=E^e_{ijkl}\ D^e_{kl}, \tag{8}$$

where

$$E^e_{ijkl}=\left(\tilde{K}-\frac{2}{3}\tilde{G}\right)\delta_{ij}\delta_{kl}+\tilde{G}(\delta_{ik}\delta_{jl}+\delta_{il}\delta_{jk}).$$

The plastic part of stretching tensor $\boldsymbol{D}^p$ is expressed as

$$D_{ij}{}^p\begin{cases}=\Lambda N_{ij}\ \text{if}\ f=0\ \text{with}\ N_{ij}\dot{T}'_{ij}>0,\\=0\ \text{if}\ f<0,\ \text{or if}\ f=0\ \text{with}\ N_{ij}\dot{T}'_{ij}\leqq0.\end{cases} \tag{9}$$

Here, noting that $N_{ij}\dot{T}'_{ij}=N_{ij}\overset{\circ}{T}{}'_{ij}$ holds, we get a scalar function Λ by Eqs. (1), (7) with $f=0$, (8), and $(9)_1$ as

$$\Lambda=\frac{E^e_{ijkl}N_{ij}D_{kl}}{E^e_{ijkl}N_{ij}N_{kl}-N_{kk}}.$$

Finally, Eqs. (1), (8), and $(9)_1$ provide a complete set of Cam-clay constitutive relations for finite plastic deformations in the form

$$\overset{\circ}{T}{}'_{ij}=\left\{\left(\tilde{K}-\frac{2}{3}\tilde{G}\right)\delta_{ij}\delta_{kl}+\tilde{G}(\delta_{ik}\delta_{jl}+\delta_{il}\delta_{jk})-\frac{\left(\frac{\tilde{G}}{\bar{\tau}}S_{ij}-\tilde{K}\bar{\beta}\delta_{ij}\right)\left(\frac{\tilde{G}}{\bar{\tau}}S_{kl}-\tilde{K}\bar{\beta}\delta_{kl}\right)}{\tilde{G}+\tilde{K}\bar{\beta}^2+h}\right\}D_{kl}, \tag{10}$$

where $\bar{\beta}=\beta/\sqrt{3}$, $\bar{\tau}=\|\boldsymbol{S}\|/\sqrt{2}$, and h is the *hardening modulus* given by

$$h=\frac{p'\bar{\beta}}{\sqrt{3}\,D},$$

hence, the Cam-clay model is a hardening material up to a critical state $\beta=0$.

Non-coaxial Cam-Clay Model

Introducing Eq. (9) into Eq. (7), we obtain

$$2D^{*p}{}_{ij}=\frac{1}{h}\frac{S_{ij}}{\bar{\tau}}\left(\frac{S_{kl}}{2\bar{\tau}}\overset{\circ}{T}{}'_{kl}-\bar{\beta}\frac{\overset{\circ}{T}{}'_{kk}}{3}\right),$$
$$D^p{}_{kk}=-\frac{\bar{\beta}}{h}\left(\frac{S_{kl}}{2\bar{\tau}}\overset{\circ}{T}{}'_{kl}-\bar{\beta}\frac{\overset{\circ}{T}{}'_{kk}}{3}\right),$$

where $\boldsymbol{D}^{*p}$ is the deviatoric part of $\boldsymbol{D}^p$. Since the principal directions of $\boldsymbol{D}^{*p}$ are coaxial with the principal directions of $\boldsymbol{S}$, we call the above constitutive relations the *coaxial Cam-clay model.*

It is well known, however, that the predictions of the initiation of shear bands in metal based on the coaxial (flow theory) model with the smooth yield surface are not in accordance with experiments (see e. g., Anand and Spitzig, 1980). In order to obtain the reasonable predictions, a number of writers then propose the non-coaxial (flow theory) models with a vertex-like theory (see e. g., Rudnicki and Rice, 1975 ; Stören, and Rice, 1975 ; Iwakuma and Nemat-Nasser, 1982 ; Gotoh, 1985). It is also argued in granular materials that the existence of microscopic localized deformations may result in such non-coaxiality (see, Mehrababi and Cowin, 1980 ; Anand, 1983).

Since our final purpose is also to simulate the formation of such localized shear bands in soils without introducing any initial imperfections in the material elements, it seems necessary to incorporate a non-coaxial term in the coaxial model. Our numerical examples in a separate paper (Yatomi et al., 1989) actually demonstrates the localized shear bands could not observed in the extended coaxial Cam-clay model. However, since we don't have reliable experimental data for such non-coaxiality in soils, we here make a model simply following the basic procedure of Rudnicki and Rice (1975). In the next section, we examine in detail the effects of non-coaxiality on the formation of shear bands.

Rudnicki and Rice (1975) consider an additional (non-coaxial) term to $\boldsymbol{D}^{*p}$, which is work-less and, therefore, makes no contribution to the rate of plastic energy loss as

$$2D^{*p}_{ij}=\frac{1}{h}\frac{S_{ij}}{\bar{\tau}}\left(\frac{S_{kl}}{2\bar{\tau}}\mathring{T}'_{kl}-\bar{\beta}\frac{\mathring{T}'_{kk}}{3}\right)+\frac{1}{h_1}\left(\mathring{S}_{ij}-\frac{S_{ij}S_{kl}}{2\bar{\tau}^2}\mathring{S}_{kl}\right). \qquad (11)$$

Here h_1 is the *second hardening modulus*, which is, for simplicity, assumed in the similar form as the hardening modulus h as

$$h_1=\frac{p'\bar{\beta}}{\sqrt{3}A} \quad (>0), \qquad (12)$$

where A is a positive material constant.

As a result, the effect of incorporating the modulus h_1 is merely exchanging the coefficients in Eqs. (10) as

$$\left.\begin{aligned}
&\tilde{G}\rightarrow\frac{h_1\tilde{G}}{h_1+\tilde{G}}=\frac{\dfrac{p'\bar{\beta}}{\sqrt{3}A}}{\dfrac{p'\bar{\beta}}{\sqrt{3}A}+\tilde{G}}\tilde{G},\\
&\tilde{K}\rightarrow\frac{(h_1-h)\tilde{K}}{h_1-h-\bar{\beta}^2\tilde{K}}=\frac{1}{1-\dfrac{\bar{\beta}^2\tilde{K}}{h_1-h}}\tilde{K},\\
&h\rightarrow\frac{h_1h}{h_1-h}=\frac{D}{D-A}h,\\
&\text{and}\\
&\bar{\beta}\rightarrow\frac{h_1\bar{\beta}}{h_1-h}=\frac{D}{D-A}\bar{\beta}.
\end{aligned}\right\} \qquad (13)$$

CONDITIONS FOR SHEAR BANDS FORMATION UNDER UNDRAINED PLANE STRAIN

Cam-clay model in Eq. (10) is a compressible material. The theoretical conditions on the shear band bifurcations for a compressible material are not, however, very simple (see e.g., Rudnicki and Rice, 1975). We then find that confining the deformation to undrained plane strain conditions makes the discussion exactly the same simple one as developed for an incompressible material by Hill and Hutchinson (1975).

Field Equations and Classification of Regimes

In equilibrium and in the absence of body forces the *surface traction vector* $\boldsymbol{t}$ must satisfy at each time

$$\int_a \boldsymbol{t}\,da=0, \qquad (14)$$

for any closed surface a. Using then the divergence theorem and a relation $\boldsymbol{t}=\boldsymbol{T}\boldsymbol{n}$ with $\boldsymbol{n}$ as an outward unit normal to a, we obtain the well known equilibrium equation

$$div\,\boldsymbol{T}=0. \qquad (15)$$

Noting that $\dot{\overline{da}}=(tr\boldsymbol{D}-\boldsymbol{n}\cdot\boldsymbol{D}\boldsymbol{n})da$ (see, Appendix 2), the differentiation of Eq. (14) with respect to time t yields

$$\int_a \dot{\boldsymbol{s}}\,da=0, \qquad (16)$$

where $\dot{\boldsymbol{s}}=\dot{\boldsymbol{t}}+(tr\boldsymbol{D}-\boldsymbol{n}\cdot\boldsymbol{D}\boldsymbol{n})\boldsymbol{t}$ is called the *total nominal traction-rate* and $\dot{\boldsymbol{S}}_t$ defined by

$$\dot{\boldsymbol{s}}=\dot{\boldsymbol{S}}_t\boldsymbol{n}$$

is the *total nominal stress-rate* ; thus $\dot{\boldsymbol{S}}_t$ is given by

$$\begin{aligned}\dot{\boldsymbol{S}}_t&=\dot{\boldsymbol{T}}-\boldsymbol{T}\boldsymbol{L}^T+(tr\boldsymbol{D})\boldsymbol{T},\\ \text{or}\quad &=\mathring{\boldsymbol{T}}+\boldsymbol{T}(tr\boldsymbol{D})-\boldsymbol{T}\boldsymbol{D}+\boldsymbol{W}\boldsymbol{T}.\end{aligned}$$

Since then $\boldsymbol{T}=\boldsymbol{T}'-u\boldsymbol{1}$ and, therefore, $\dot{\boldsymbol{T}}=\dot{\boldsymbol{T}}'-\dot{u}\boldsymbol{1}$, we note that for saturated clays the total nominal stress-rate $\dot{\boldsymbol{S}}_t$ is related to the *effective nominal stress-rate* $\dot{\boldsymbol{S}}_t'$ as

$$\dot{\boldsymbol{S}}_t=\dot{\boldsymbol{S}}_t'-\dot{u}\boldsymbol{1}-u(tr\boldsymbol{D})\boldsymbol{1}+u\boldsymbol{L}^T, \qquad (17)$$

where $\dot{\boldsymbol{S}}_t'$ is defined by

$$\dot{S}_t' = \overset{\circ}{T}' + T'(trD) - T'D + WT'. \qquad (18)$$

Using the divergence theorem in Eq. (16), we finally obtain the continuing equilibrium equation

$$div\dot{S}_t = 0. \qquad (19)$$

Note that Eq. (19) is also a direct result of the material time derivative of Eq. (15).

In what follows, we confine our attention to a study of the formation of shear bands under *quasi-static undrained plane strain* conditions in the absence of body forces. We consider a pure homogeneous plane deformation process which starts from an isotropically consolidated state ; at any time thereafter, up to the instant of shear band formation the state of uniform stress is assumed and the directions of the coordinates x_1 x_2 and x_3 are conincident with the principal stress axes.

In terms of the effective co-rotational rate of the Cauchy stress T', and the stretching D, the constitutive relations Eq. (10) for continuing undrained plastic loading may be then written as

$$\left.\begin{aligned} \overset{\circ}{T}'_{11} - \overset{\circ}{T}'_{22} &= 2\mu^*(D_{11} - D_{22}), \\ \overset{\circ}{T}'_{12} &= 2\mu D_{12}, \end{aligned}\right\} \qquad (20)$$

with

$$D_{11} + D_{22} = 0 \text{ and } D_{33} = 0.$$

Here the *instantaneous shear moduli* μ^* and μ are given in the form

$$\mu^* = \frac{\tilde{G}\tilde{h}}{\tilde{G} + \tilde{h}},$$

with

$$\tilde{h} = \tilde{K}\bar{\beta}^2 + h,$$

and

$$\mu = \tilde{G}.$$

Since our constitutive relations Eq. (20) and the continuing equilibrium equation Eq. (19) under undrained plane strain conditions are exactly the same ones that Hill and Hutchinson (1975) developed for an incompressible material, we here simply follow their results.

Let (v_1, v_2) be the (x_1, x_2) components of velocity and introduce a stream function $\Psi(x_1, x_2)$ such that

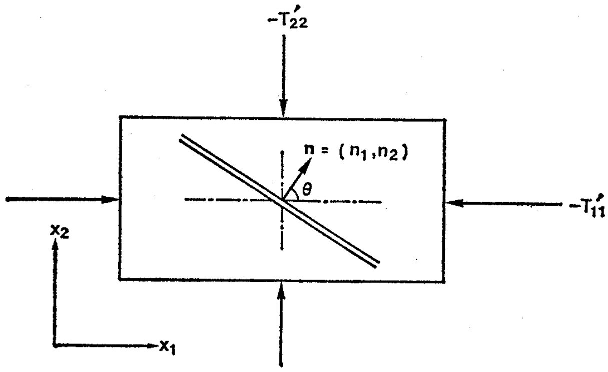

Fig. 1. Inclination of a shear band

$$v_1 = \frac{\partial \Psi}{\partial x_2}, \quad v_2 = -\frac{\partial \Psi}{\partial x_1}.$$

Substituting Eq. (17) with Eq. (18), and Eq. (20) into Eq. (19), with the assumptions that the current stress is uniform and undrained conditions $trD = 0$, we have

$$(\mu + \tau)\frac{\partial^4 \Psi}{\partial x_1^4} + 2(2\mu^* - \mu)\frac{\partial^4 \Psi}{\partial x_1^2 \partial x_2^2} + (\mu - \tau)\frac{\partial^4 \Psi}{\partial x_2^4} = 0, \qquad (21)$$

where we put

$$\tau = \frac{T'_{11} - T'_{22}}{2} \text{ or } \frac{S_{11} - S_{22}}{2}.$$

With n denoting an unit vector normal to a shear band(see, Fig. 1), Hill and Hutchinson (1975) then introduce a velocity field for which the stream function is of type

$$\Psi = F(n_1 x_1 + n_2 x_2) \qquad (22)$$

which represents an inhomogeneous simple shear parallel to planes $n_1 x_1 + n_2 x_2 =$ constant.

Introducing Eq. (22) into Eq. (21), then obtain a characteristic equation

$$(\mu + \tau)n_1^4 + 2(2\mu^* - \mu)n_1^2 n_2^2 + (\mu - \tau)n_2^4 = 0. \qquad (23)$$

The elliptic (E), parabolic (P), and hyperbolic (H) regimes are identified depending on whether there are 0, 2, or 4 real values of n_2/n_1, respectively, that satisfy Eq. (23) ; they are classified as follows under the restrictions

$$\mu^* > 0, \ \mu > 0, \ \tau > 0 :$$

$$E : 2\mu^* > \mu - \sqrt{\mu^2 - \tau^2},$$

$$H: 2\mu^* < \mu - \sqrt{\mu^2 - \tau^2},$$
$$P: \mu < \tau.$$

An overview of these regimes is shown in Fig. 3.

Effects of the Non-coaxial Term on Shear Bands Formation

Here we examine the effects of the non-coaxial term on shear bands formation. The discussions and the numerical examples are confined to the constitutive relations Eq. (11) with the second hardening modulus h_1 in the form of Eq. (12).

(1) *Effects on the instantaneous shear moduli*

When the non-coaxial term is incorporated as Eq. (11), $\tilde{G}$, $\tilde{K}$, h, and $\bar{\beta}$ change their forms as Eq. (13) ; hence,

$$\tilde{h} = \tilde{K}\bar{\beta}^2 + h \rightarrow \frac{h_1 \tilde{h}}{h_1 - \tilde{h}},$$

and therefore

$$\mu^* = \frac{\tilde{G}\tilde{h}}{\tilde{G} + \tilde{h}}$$
$$\rightarrow \frac{\dfrac{h_1\tilde{G}}{h_1+\tilde{G}} \dfrac{h_1\tilde{h}}{h_1-\tilde{h}}}{\dfrac{h_1\tilde{G}}{h_1+\tilde{G}} + \dfrac{h_1\tilde{h}}{h_1-\tilde{h}}} = \frac{\tilde{G}\tilde{h}}{\tilde{G}+\tilde{h}},$$

that is, μ^* is independent of the non-coaxial term.

On the other hand, Eq. $(13)_1$ shows that

$$\mu = \tilde{G} \rightarrow \frac{h_1\tilde{G}}{h_1+\tilde{G}} \ (<\tilde{G}),$$

that is, the incorporating the modulus h_1 makes the value of μ smaller.

Thus we conclude that the incorporating the non-coaxial term has no effect on the instantaneous shear modulus μ^* for the normal effective stress difference $T'_{11} - T'_{22}$ and it makes the instantaneous shear modulus μ for the shear stress T'_{12} smaller. Here we set $\alpha = q/Mp'$; thus,

$$\bar{\beta} = \frac{\beta}{\sqrt{3}} = \frac{M(1-\alpha)}{\sqrt{3}}.$$

Note that $0 \leqq \alpha \leqq 1$; $\alpha = 0$ corresponds to the initial isotropically consolidated state and

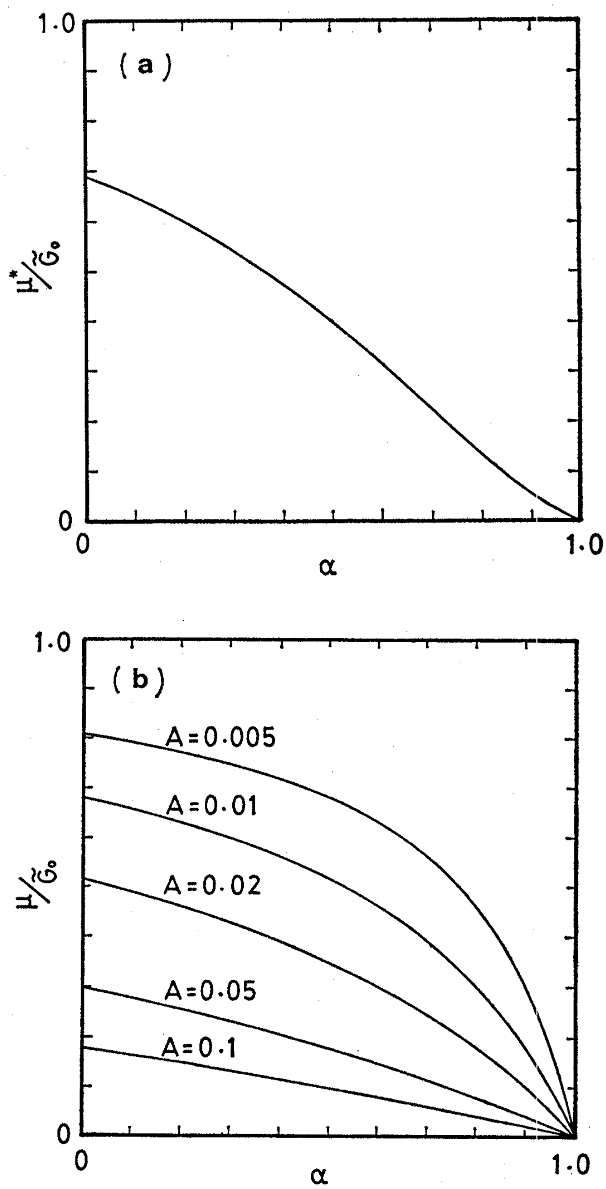

Fig. 2. Curves of the instantaneous shear moduli vs. α

$\alpha = 1$ the critical state.

The instantaneous shear moduli μ^* and μ are then both monotone decreasing function on α ; see Fig. 2, in which $\tilde{G}_0$ is the shear modulus in the case of coaxial model. We find that, as we expected, the bigger A makes μ smaller.

Here and in what follows, the soil parameters are taken to be

$$\lambda = 0.231,$$
$$\kappa = 0.042,$$
$$\nu = 0.333, \qquad (24)$$

$$M=1.430,$$

and

$$e=1.5\ (=e_0),\ (\therefore\ D=0.053),$$

which are determined from the experimental results on triaxial tests of Umeda Clay, reported by Sekiguchi (1977).

(2) *Effect on the behavior in the characteristic regimes*

For a given constitutive relation Eq. (10) it is not difficult to show that if $2T'_{33}=T'_{11}+T'_{22}$ initially, the same relation holds for any time ; the initial isotropically consolidated state satisfies its relation.

Since then $S_{11}=\tau$, $S_{22}=-\tau$, and $S_{33}=0$, we have

$$\bar{\tau}=|\tau| \text{ and } q=\sqrt{3}|\tau| ;$$

hence

$$\tau=\frac{Mp'}{\sqrt{3}}\alpha \text{ if } \tau>0.$$

We then obtain the trajectories of $(\tau/2\mu^*.\ \mu/2\mu^*)$ for $0\leqq\alpha\leqq1$ (see Fig. 3). Note that

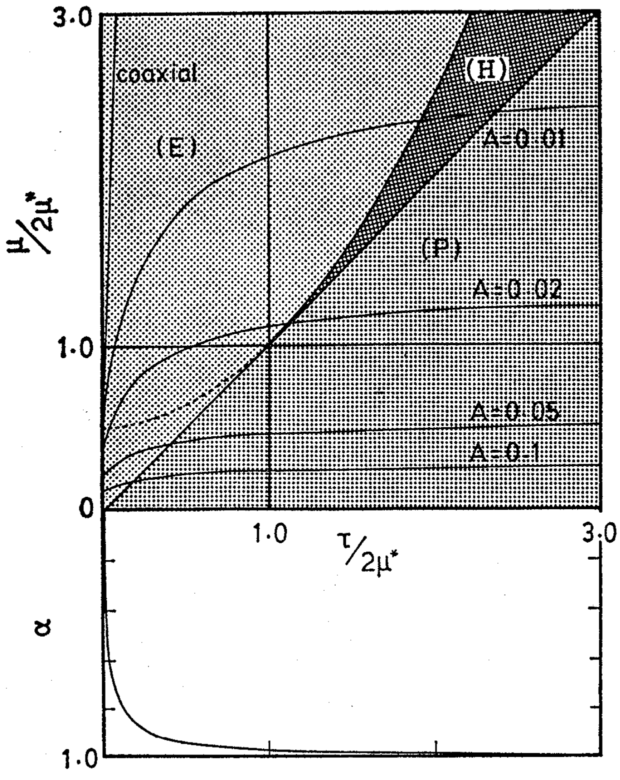

Fig. 3. Trajectories of $(\tau/2\mu,\ \mu/2\mu^*)$ and the dependence of $\tau/2\mu^*$ on α

$$\frac{\tau}{2\mu^*}\to\infty,$$

$$\frac{\mu}{2\mu^*}\to\frac{D}{2A},$$

as $\alpha\to1$.

For $A=0.01$, the trajectory is $(E)\to(H)\to(P)$, but for $A=0.05$, it passes directly into (P) from (E).

The dependence of $\tau/2\mu^*$ on α in Fig. 3 shows that when the trajectory passes the E/H boundary α is nearly 1, that is, the stress state is very close to the critical state ; moreover, the smaller A becomes, the more α is close to 1.

(3) *Effects on the accessibility to the transition boundary and the angle of shear band inclination at the boundary*

Here we examine in detail the effect of non-coaxial term. When the trajectory passes the E/H boundary we have

$$\tau^2=4\mu^*(\mu-\mu^*) \tag{25}$$

with

$$\mu/2\mu^*>1.$$

Using Eq. (25) with the soil parameters in Eq. (24), we obtain the exact dependence of α on A when the trajectory passes the E/H boundary (see Fig. 4). We then find that the non-coaxial term makes easy of access to

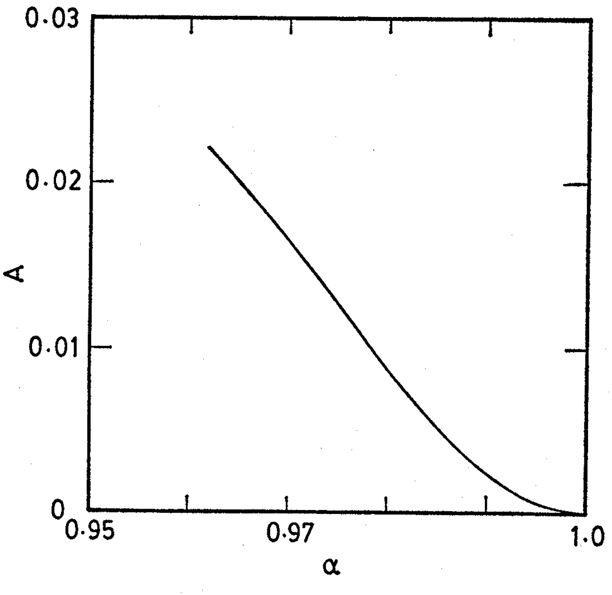

Fig. 4. A vs. α when the trajectory passes the E/H boundary

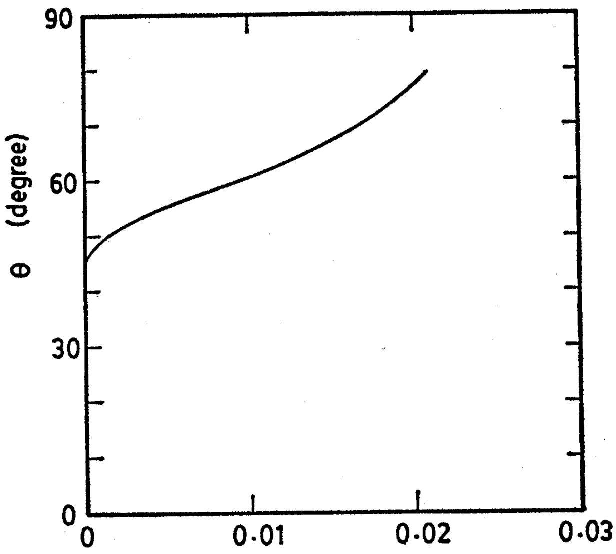

Fig. 5. Inclination of the shear band vs. *A* when the trajectory passes the *E/H* boundary

the E/H boundary. For a coaxial model with $A=0$, we have $\alpha \fallingdotseq 1$ when the trajectory passes the E/H boundary; namely, the stress state is on the critical state.

If a shear band occurs at the instant when the trajectory passes the E/H boundary, the angle of shear band inclination is given by a solution of Eq. (23) as

$$\left(\frac{n_2}{n_1}\right)^2=\frac{\mu-2\mu^*}{\mu-\tau}.$$

Fig. 5 shows that the inclination angle $\theta(=\tan^{-1}(n_2/n_1))$ of the shear band to the maximum (effective) principal compressive stress (see Fig. 1) is bigger than $\pi/4$ and the angle becomes bigger with the bigger A.

Consider an example for $A=0.05$ in Fig. 3; the trajectory passes directly into (P) from (E). At the instant when it passes the E/P boundary, we have

$$\mu=\tau;$$

hence, by Eq. (23) $n_1=0$. That is, the direction of shear band inclination is perpendicular to the maximum (effective) principal compressive stress, which seems to be unrealistic.

(4) *Effect on simple shearing modulus*

Most theoretical analyses on the shear band bifurcation (e.g., Rudnicki and Rice, 1975; Stören and Rice, 1975; Anand and Spitzig, 1980) are, as stated above, confined to the discussion at the instant of a failure of ellipticity under the uniform field. Moreover, it is nothing but a necessary condition for the existence of shear bands as the discontinuity of strain-rate. However, for the non-uniform fields under the actual given boundary value problems, even the material elements in elliptic regime may have some effects on the accessibility to shear bands formation. Even if we observe the shear bands formation in finite element deformed meshes, in which shear strains grow locally very large, the continuing equilibrium equation in that region may still be elliptical.

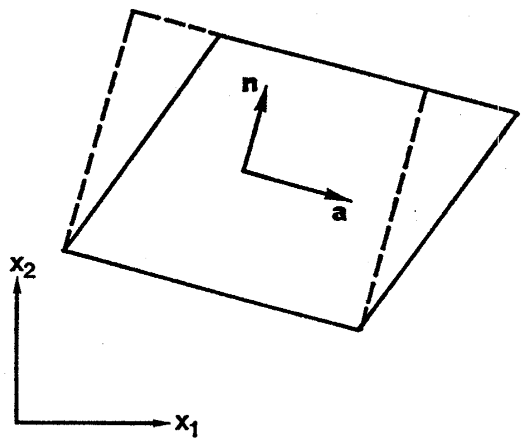

Fig. 6. Simple shearing

We then propose a new measure to see the accessibility to shear bands formation. Consider a simple shearing $\boldsymbol{L}=\boldsymbol{a}\otimes\boldsymbol{n}$ with $\boldsymbol{n}=(n_1, n_2)$ as an arbitrary unit vector (which, in general, has nothing to do with shear bands inclination) and $\boldsymbol{a}=(n_2, -n_1)$ the unit normal vector to $\boldsymbol{n}$ (see Fig. 6). Note that we here confine our discussion to deformation under the undrained condition; i.e. $tr\boldsymbol{D}=\boldsymbol{a}\cdot\boldsymbol{n}=0$.

Then if

$$g=\dot{\boldsymbol{S}}_t\cdot\boldsymbol{L}>0$$

holds for all (rank one) tensors $\boldsymbol{L}=\boldsymbol{a}\otimes\boldsymbol{n}$, it is called the *strong ellipticity condition* (see e.g., Ogden, 1984). If there exists $\boldsymbol{n}$ such that $g=0$, the continuing equibulium equation ceases to be elliptic and becomes parabolic or hyperbolic. In fact, noting that $\mathbf{1}\cdot\boldsymbol{L}=0$ and $\boldsymbol{L}^T\cdot\boldsymbol{L}=0$ for $\boldsymbol{L}=\boldsymbol{a}\otimes\boldsymbol{n}$, we easily find that

$$
\begin{aligned}
g&=\dot{\boldsymbol{S}}_t\cdot\boldsymbol{L},\\
&=\dot{\boldsymbol{S}}_t{}'\cdot\boldsymbol{L},\\
&=(\mu+\tau)n_1{}^4+2(2\mu^*-\mu)n_1{}^2n^2{}_2+(\mu-\tau)n_2{}^4,
\end{aligned}
$$

which is exactly the same as the left-hand side of Eq. (23).

This motivates us that the positive magnitude of g reveals a distance from the E/P or E/H boundary, in other words, from a necessary condition for the existence of shear bands. Since here $\boldsymbol{L}=\boldsymbol{a}\otimes\boldsymbol{n}$ is a simple shearing and then $g=\dot{\boldsymbol{S}}_t\cdot\boldsymbol{L}$ is a kind of rigidity for the shearing, we call g the *simple shearing modulus.*

Let $n_1=\cos\theta$ and $n_2=\sin\theta$; then the simple shearing modulus

$$
g(\theta;\alpha,A)=(\mu-\mu^*)\cos^2 2\theta+\tau\cos 2\theta+\mu^*, \qquad (26)
$$

may be regarded as a function of the shearing angle θ with parameters α and A.

We note that, in particular,

$$
g(0;\alpha,A)=\mu+\tau,
$$

$$
g\left(\frac{\pi}{2};\alpha,A\right)=\mu-\tau,
$$

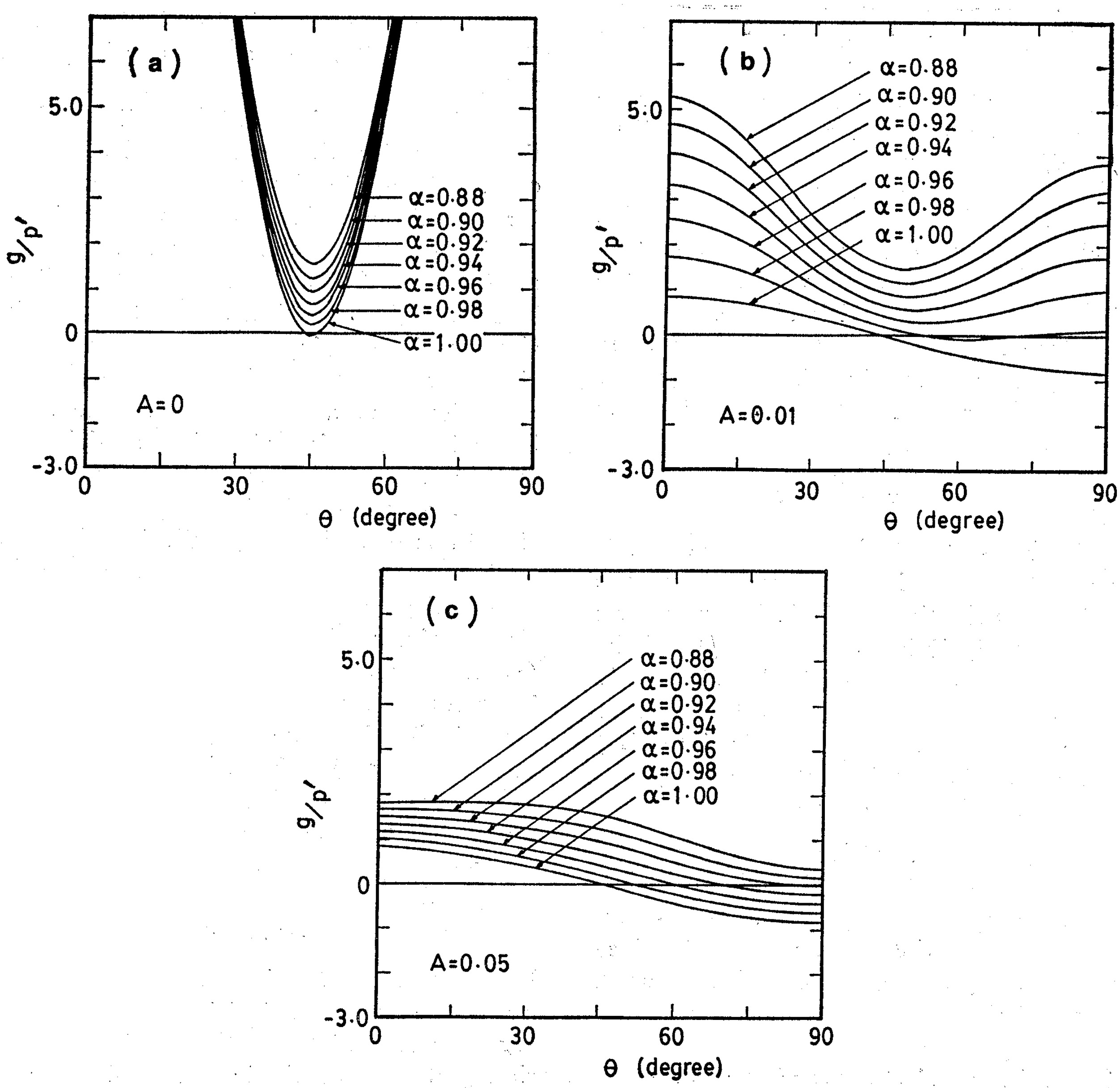

Fig. 7. Simple shearing modulus vs. shearing angle θ with parameter α

and

$$g\left(\frac{\pi}{4}\,;\,\alpha, A\right)=\mu^*,$$

where μ^* is independent of A.

Since $\tau=0$ in Eq. (26) for small strain theory, introducing the relations $\mu^*=\tilde{G}\tilde{h}/(\tilde{G}+\tilde{h})$ and $\mu=\tilde{G}$ into Eq. (26), we have

$$g=\frac{\tilde{G}}{\tilde{G}+\tilde{h}}(\tilde{G}\cos^2 2\theta+\tilde{h})\ ;$$

hence, if the shear modulus $\tilde{G}>0$, the shear bands as the discontinuity of strain rate can not occur in the hardening material $\tilde{h}>0$.

In Fig. 7, g/p' is plotted in the neighborhood of critical state $\alpha=0.88\sim1.00$ for $A=0$, 0.01 and 0.05 with the soil parameters in Eq. (24). Here we may observe the transition of the characteristic regimes in Fig. 3 from the simple shearing modulus viewpoint. The shearing angle θ which has the minimum value of g/p' may be the direction which is most easy to deform in shear. We find that for $A=0$, i. e. for a coaxial model, g/p' is relatively large except around $\theta\fallingdotseq\pi/4$. For $A=0.01$ and 0.05, i. e. for non-coaxial models, g/p' becomes smaller for all θ ($0\leqq\theta\leqq\pi/2$) than for $A=0$, even before g/p' reaches to zero. This predicts, in the neighborhood of critical state, that the non-coaxial models are easier to deform in shear for any directions than the coaxial model ; therefore, the non-coaxial model are, independently of the kinematic constraint, more inclined to instability by localization of deformation than the coaxial model.

CONCLUSION

We first present a systematic extension of the well known Cam-clay model developed for small strains to the model for finite strains. We then propose a new model which incorporates a non-coaxial term in the extended Cam-clay model. Finally, confining the deformation to undrained plane strain conditions, we examine the effects of the non-coaxial term on the shear bands formation. As a result, we conclude :

1) The incorporation of the non-coaxial term has no effect on the instantaneous shear modulus for the normal stress difference and it makes the instantaneous shear modulus for the shear stress smaller ;

2) The non-coaxial term makes easy of access to the elliptic/hyperbolic boundary ;

3) The behavior of the simple shearing modulus, which is proposed here as a new measure to see the accessibility to shear bands formation, shows that, in the neighborhood of critical state, the non-coaxial models are, independently of the kinematic constraint, more inclined to instability by localization of deformation than the coaxial model.

ACKNOWLEDGEMENTS

We wish to express our gratitude for the encouragement received from Professor Hideki Ohta of Kanazawa University. We also wish to express our thanks to Professor Fumio Tatsuoka of Tokyo University for kindly permitting us to quote a photo obtained from their experiment. Acknowledgement also is due to Mr. Sumio Sawada of Osaka Geo Research Institute. This study was supported in part by a Grant-in-Aid for Science Research, Project No. 63302045 from the Ministry of Education, Science and Culture.

NOTATION

A = positive material constant indicated non-coaxiality
$\boldsymbol{a}$ = unit normal vector to $\boldsymbol{n}$
D = coefficient of dilatancy
$\boldsymbol{D}$ = stretching tensor
$\boldsymbol{D}^e$ = elastic part of the stretching tensor
$\boldsymbol{D}^p$ = plastic part of the stretching tensor
$\boldsymbol{D}^{*p}$ = deviatoric part of $\boldsymbol{D}^p$
$d\boldsymbol{a}, d\boldsymbol{A}$ = area vectors at the current and reference time, respectively
$E^e{}_{ijkl}$ = elastic stiffness
e, e_0 = void ratio at the current and reference time, respectively
$\boldsymbol{F}$ = deformation gradient
f = yield functional
$\tilde{G}$ = shear modulus
$\tilde{G}_0$ = shear modulus in the case of the coaxial model

g=simple shearing modulus
h=hardening modulus
h_1=second hardening modulus
J=Jacobian of $\boldsymbol{F}$
$\tilde{K}$=bulk modulus
$\boldsymbol{L}$=velocity gradient
$\boldsymbol{n}$=unit normal vector
$(n_1, n_2)=(x_1, x_2)$ components of $\boldsymbol{n}$
p'=effective mean normal stress
q=generalized stress deviator
$\boldsymbol{S}$=deviatoric part of $\boldsymbol{T}'$
$\dot{\boldsymbol{S}}_t$=total nominal stress-rate
$\dot{\boldsymbol{S}}_t'$=effective nominal stress-rate
$\dot{\boldsymbol{s}}$=total nominal stress traction rate
$\boldsymbol{T}$=total Cauchy stress tensor
$\boldsymbol{T}'$=effective (Cauchy) stress tensor
$\overset{\circ}{\boldsymbol{T}}'$=co-rotational (Jaumann) rate of effective stress
t=time
$\boldsymbol{t}$=surface traction vector
u=pore water pressure
v=volumetric strain
$\dot{v}^p$=volumetric plastic strain rate
$(v_1, v_2)=(\dot{x}_1, \dot{x}_2)$ components of velocity
$\boldsymbol{x}, \boldsymbol{X}$=material point in the current state and in the reference state, respectively
$\boldsymbol{W}$=spin tensor
$\boldsymbol{1}$=unit tensor
$\alpha=q/Mp'$
$\beta=M-\eta$
$\bar{\beta}=\beta/\sqrt{3}$
$\delta_{ij}=i, j$ component of Kronecker's delta
η=stress ratio $(=q/p')$
θ=shearing angle
κ=swelling index
Λ=non-negative scalar function in Eq. (9)
λ=compression index
M=critical state parameter
μ=instantaneous shear modulus for the shear stress
μ^*=instantaneous shear modulus for the normal effective stress difference
ν=Poisson's ratio
τ=normal effective stress difference in Eq. (21)
$\bar{\tau}=\|S\|/\sqrt{2}$
Ψ=stream function

REFERENCES

1) Anand, L. and Spitzig, W. A. (1980) : "Initiation of localized shear bands in plane strain," J. Mech. Phys. Solids, Vol. 28, pp. 113-128.
2) Anand, L. (1983) : "Plane deformations of ideal granular materials," J. Mech. Phy. Solids, Vol. 31, pp. 105-122.
3) Borst, R. D. (1988) : "Bifurcations in finite element models with a non-associated flow law," Int. J. Numer. and Anal. Methods Geomech., Vol. 12, pp. 99-116.
4) Eringen, A. C. (1967) : Mechanics of Continua, John Wiley & Sons, Inc.
5) Gotoh, M. (1985) : "A class of plastic constitutive equations with vertex effect - I. General theory," Int. J. Solids Structures, Vol. 21, pp. 1101-1116.
6) Hill, R. and Hutchinson, J. W. (1975) : "Bifurcation phenomena in the plane tension test," J. Mech. Phys. Solids, Vol. 23, pp. 239-264.
7) Iwakuma, T. and Nemat-Nasser, S. (1982) : "An analytical estimate of shear band initiation in a necked bar," Int. J. Solids Structures, Vol. 18, pp. 69-83.
8) Mehrababi, M. M. and Cowin, S. C. (1980) : "Prefailure and postfailure soil plasticity models," J. Engng. Mech. Div. ASCE, Vol. 106, EM 5, pp. 991-1003.
9) Ogden, R. W. (1984) : Non-linear Elastic Deformations, Ellis Horwood.
10) Ohta, H. (1971) : "Analysis of deformations of soils based on the theory of plasticity and its application to settlement of embankments," Doctor Engineering Thesis, Kyoto Univ..
11) Prevost, J. H. and Hughes, T. J. R. (1981) : "Finite-element solution of elastic-plastic boundary-value problem," J. Applied Mech., ASME, Vol. 48, pp. 69-74.
12) Prevost, J. H. (1984) : "Localization of deformations in elastic-plastic solids," Int. J. Numer. and Anal. Methods Geomech., Vol. 8, pp. 187-196.
13) Roscoe, K. H., Schofield, A. N. and Thurairajah, A. (1963) : "Yielding of clays in states wetter than critical," Geotechnique, Vol. 13, pp. 211-240.
14) Rudnicki, J. W. and Rice, J. R. (1975) : "Conditions for the localization of deformation in pressure-sensitive dilatant materials," J. Mech. Phys. Solids, Vol. 23, pp. 371-394.
15) Sekiguchi, H. (1977) : "Rheological characteristics of clays," Proc. 9 th ICSFME, Tokyo, Vol. 1, pp. 289-291.
16) Stören, S. and Rice, J. R. (1975) : "Localized necking in thin sheets," J. Mech. Phys. Solids, Vol. 23, pp. 421-441.
17) Tani, K., Tatsuoka, F. and Mori, H. (1987) : "Effects of pressure level and model site on bearing capacity of model strip footing on

sand," Proc. 22 th Japan National Conf. Soil Mechanics and Foundation Engineering, Vol. 2-2, pp. 1091-1094 (in Japanese).

18) Yatomi, C., Yashima, A., Iizuka, A. and Sano, I. (1989) : "Shear bands formation numerically simulated by a noncoaxial Cam-clay model," Soils and Foundations (to appear).

APPENDIX 1

Mathematical Symbols

Light-face letters indicate scalars ; bold-face letters indicate vectors or tensors ; we use standard indicial notation and Cartesian coordinates, x_i, $i=1,2,3$. If $\boldsymbol{A}$, $\boldsymbol{B}$ are second order tensor and $\boldsymbol{a}$, $\boldsymbol{b}$ are vectors,

$\boldsymbol{A}^T$ is the transpose of $\boldsymbol{A}$,

$\boldsymbol{A}^{-1}$ is the inverse of $\boldsymbol{A}$,

$$(\boldsymbol{AB})_{ij}=A_{ik}B_{kj},$$

$$tr\boldsymbol{A}=A_{kk},$$

$$\boldsymbol{A}\cdot\boldsymbol{B}=tr(\boldsymbol{AB}^T)=A_{ij}B_{ij},$$

$$\|\boldsymbol{A}\|=\sqrt{tr(\boldsymbol{AA}^T)},$$

$$(\boldsymbol{Ab})_i=A_{ij}b_j,$$

$$\boldsymbol{a}\cdot\boldsymbol{b}=a_ib_i,$$

and

$$(\boldsymbol{a}\otimes\boldsymbol{b})_{ij}=a_ib_j.$$

If $\boldsymbol{A}$ is defined in a field,

$$(div\boldsymbol{A})_i=A_{ij,j}=\partial A_{ij}/\partial x_j.$$

APPENDIX 2

Let $d\boldsymbol{a}$ and $d\boldsymbol{A}$ be the area vectors at the current and reference time, respectively.

Since then

$$d\boldsymbol{a}=J\boldsymbol{F}^{-T}d\boldsymbol{A}$$

(see e.g., Eringen, p. 46), material time derivative of

$$da^2:=d\boldsymbol{a}\cdot d\boldsymbol{a}=J^2\boldsymbol{F}^{-T}d\boldsymbol{A}\cdot\boldsymbol{F}^{-T}d\boldsymbol{A}$$

becomes

$$2\,da\dot{\overline{da}}=\frac{2\dot{J}}{J}(da)^2+2J^2(\boldsymbol{F}^{-T})^{\cdot}d\boldsymbol{A}\cdot\boldsymbol{F}^{-T}d\boldsymbol{A},$$

$$=\frac{2\dot{J}}{J}(da)^2+2(\boldsymbol{F}^{-T})^{\cdot}\boldsymbol{F}^Td\boldsymbol{a}\cdot d\boldsymbol{a},$$

$$=\frac{2\dot{J}}{J}(da)^2-2\,\boldsymbol{L}^Td\boldsymbol{a}\cdot d\boldsymbol{a},$$

$$=2(tr\boldsymbol{D}-\boldsymbol{n}\cdot\boldsymbol{Dn})(da)^2,$$

which yields the final result.